



MOX-Report No. 34/2015

**A separable model for spatial functional data with  
application to the analysis of the production of waste in  
Venice province**

Bernardi, M.S.; Mazza, G.; Ramsay, J.O.; Sangalli, L.M.

MOX, Dipartimento di Matematica  
Politecnico di Milano, Via Bonardi 9 - 20133 Milano (Italy)

[mox-dmat@polimi.it](mailto:mox-dmat@polimi.it)

<http://mox.polimi.it>

# A separable model for spatial functional data with application to the analysis of the production of waste in Venice province

Mara S. Bernardi<sup>1</sup>      Gabriele Mazza<sup>1</sup>      James O. Ramsay<sup>2</sup>  
Laura M. Sangalli<sup>1</sup>

<sup>1</sup> MOX - Department of Mathematics, Politecnico di Milano, Piazza Leonardo da Vinci 32, 20133, Milano, Italy, (e-mail: [laura.sangalli@polimi.it](mailto:laura.sangalli@polimi.it))

<sup>2</sup> Department of Psychology, McGill University, Montréal, Canada

## Abstract

We propose a method for the analysis of functional data with complex dependencies, such as spatially dependent curves or time dependent surfaces, over highly textured domains. The models are based on the idea of regression with partial differential regularizations. We focus in particular on a separable space-time version of the model. Among the various modelling features, the proposed method is able to deal with spatial domains featuring peninsulas, islands and other complex geometries. Space-varying covariate information is included in the model via a semi-parametric framework. The proposed method is compared via simulation studies to other spatio-temporal techniques and it is applied to the analysis of the annual production of waste in the towns of Venice province.

**Keywords:** Space-time model; Differential regularization; Finite elements

## 1 Introduction

In this work we deal with spatio-temporal data distributed over a spatial domain which presents complex geometries. That is, the irregular shape of the domain influences the phenomenon under study and there are important geographical elements within the boundary such as islands and peninsulas that impact the distribution of the data. We refer to such domains as *textured*.

As an illustrative example, consider the estimation of the temporal evolution of the amount of per capita municipal waste produced in the towns of Venice province. Figure 1 shows the Venice province, with dots indicating town centers, including municipalities and other tourist localities of particular relevance. The province boundary is shown by a red line, highlighting the irregular shape of the province geographical borders and its complex coastlines, with the Venice lagoon partly enclosed by elongated peninsulas and small islands.

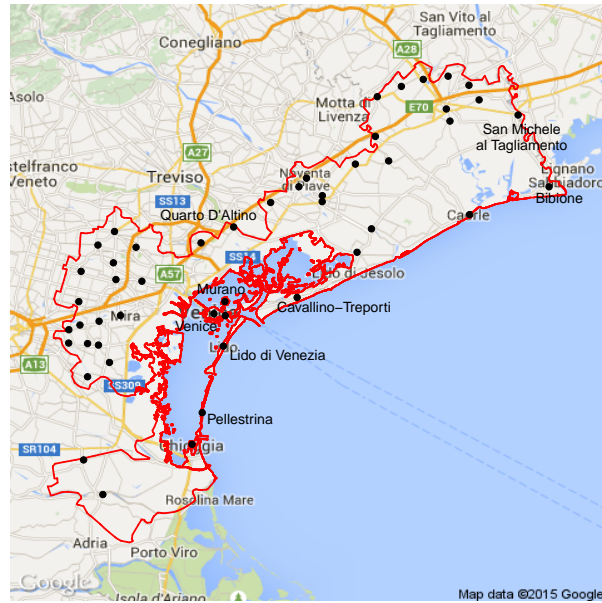


Figure 1: Spatial domain and locations of the Venice waste data with the province boundary shown by the red line.

The data are measurements from 1997 to 2011 of the yearly amount of per capita municipal waste (total kg divided by the number of municipality residents) and are provided by the Arpav, the Agenzia regionale per la prevenzione e protezione ambientale del Veneto. Figure 2 shows the temporal evolution of the production of per capita waste in the towns of Venice province and Figure 3 is a bubble plot of the data at a fixed year, 2006.

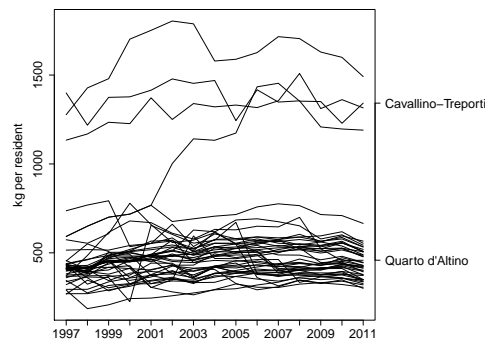


Figure 2: Temporal evolution of the yearly per capita production (kg per resident) of municipal waste in the towns of Venice province.

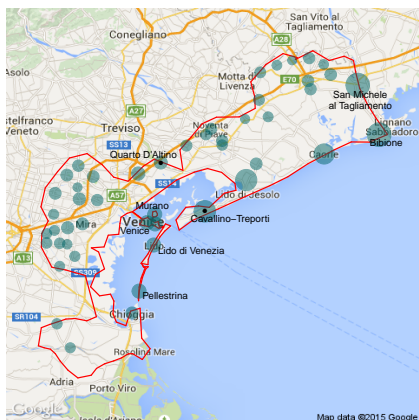


Figure 3: Per capita production (kg per resident) of municipal waste in the towns of Venice province in 2006.

The phenomenon portrayed by these data is expressed differently in different parts of the domain. Consider for instance the two towns of Cavallino-Treporti (in the peninsula at the north-east of Venice) and Quarto d'Altino (north of Venice), indicated by black dots in Figure 3. The temporal evolution of the production of per capita municipal waste in the two towns, highlighted in Figure 2, is rather different, with values high and more strongly increasing in the seaside and tourist town of Cavallino-Treporti, opposed to the lower and less strongly increasing values measured in hinterland town of Quarto d'Altino. These two towns are close in terms of their geodesic distance, but they are actually separated by the Venice lagoon. Hence, appropriately accounting for the shape of the domain, characterized for instance by a strong concavity formed by the lagoon, is crucial to accurately handle these data.

The temporal evolutions of the amount of per capita municipal waste can be considered as spatially dependent one-dimensional functional data. Various methods have been recently proposed to handle such data. Starting from the pioneering work of Goulard and Voltz [1993], kriging prediction methods for stationary spatial functional data are developed in Delicado et al. [2010], Nerini et al. [2010] and Giraldo et al. [2011]. Recent techniques developing universal kriging approaches for spatially dependent functional data are offered by Caballero et al. [2013], Menafoglio et al. [2013] and Menafoglio et al. [2014]. An extension of kriging for functional data which takes into account the presence of covariates is developed in Ignaccolo et al. [2014]. The same data can be also considered in a more classical space-time data framework. An extensive literature on spatio-temporal models has been produced; we refer the reader to Cressie and Wikle [2011] and references therein. On the other hand, these methods are not well suited for the context we are here considering because they do not take into account the shape of the domain; for instance these methods would smooth across concave boundary regions, thus closely linking data points that are in fact far apart by land connections.

Recent methods for the analysis of spatio-temporal data that instead specifically account for the the geometry of the domain of interest are described in Augustin et al. [2013] and Marra et al. [2012]. These models are based on the spatial smoother proposed by Wood et al. [2008]. Here, we extend the spa-

tial models with differential regularization described in Ramsay [2002], Sangalli et al. [2013] and Azzimonti et al. [2014] to time dependent data, and propose a Spatio-Temporal regression model with Partial Differential Equations regularization (ST-PDE). The model is implemented in R [R Core Team, 2014].

The paper is organized as follows. Section 2 describes the ST-PDE model. Section 3 shows the numerical implementation of the model. Section 4 illustrates the extension of the model for the inclusion of space-varying covariates. Section 5 compares via simulation studies the ST-PDE model to other spatio-temporal prediction techniques. Section 6 shows the application of the proposed method to the analysis of the per capita municipal waste in the Venice province. Section 7 outline some possible model extensions. Finally, some additional comments on the model are given in the Appendix.

## 2 Data and model

Let  $\{\mathbf{p}_i = (x_i, y_i); i = 1, \dots, n\}$  be a set of  $n$  spatial points on a bounded regular domain  $\Omega \subset \mathbb{R}^2$  and  $\{t_j; j = 1, \dots, m\}$  be a set of  $m$  time instants in a time interval  $[T_1, T_2] \subset \mathbb{R}$ . Let  $z_{ij}$  be the value of a real-valued variable observed at point  $\mathbf{p}_i$  and time  $t_j$ . The spatial domain  $\Omega$  is the province of Venice, the spatial locations  $\mathbf{p}_i$  are the towns, the time instants  $t_j$  are the years between 1997 and 2011 and the variable of interest  $z_{ij}$  is the amount of the annual production of per capita municipal waste in year  $t_j$  at the town location  $\mathbf{p}_i$ . The data  $z_{ij}$  are a sampling of space dependent temporal curves. Equivalently, they can be seen as a sampling of time dependent surfaces on  $\Omega$ .

We assume that  $\{z_{ij}; i = 1, \dots, n; j = 1, \dots, m\}$  are noisy observations of an underlying spatio-temporal smooth function  $f(\mathbf{p}, t)$ :

$$z_{ij} = f(\mathbf{p}_i, t_j) + \epsilon_{ij} \quad i = 1, \dots, n, \quad j = 1, \dots, m, \quad (1)$$

where  $\{\epsilon_{ij}; i = 1, \dots, n; j = 1, \dots, m\}$  are independently distributed residuals with mean zero and constant variance  $\sigma^2$ .

We use a separable model for the spatio-temporal field  $f(\mathbf{p}, t)$  by representing it as an expansion on a separable space-time basis system. We hence estimate  $f(\mathbf{p}, t)$  by minimizing a penalized sum of square error functional  $J(f)$ , where the penalization takes into account separately the regularity of the function in the spatial and temporal domains.

Specifically, let  $\{\varphi_k(t); k = 1, \dots, M\}$  be a set of  $M$  basis functions defined on  $[T_1, T_2]$  and  $\{\psi_l(\mathbf{p}); l = 1, \dots, N\}$  a set of  $N$  basis functions defined on  $\Omega$ . Then, we can express the spatio-temporal field  $f$  in the following basis expansions:

$$f(\mathbf{p}, t) = \sum_{k=1}^M a_k(\mathbf{p}) \varphi_k(t) \quad (2)$$

$$= \sum_{l=1}^N b_l(t) \psi_l(\mathbf{p}) \quad (3)$$

$$= \sum_{l=1}^N \sum_{k=1}^M c_{lk} \psi_l(\mathbf{p}) \varphi_k(t) \quad (4)$$

where  $\{a_k(\mathbf{p}); k = 1, \dots, M\}$  are the spatially varying coefficients of the expansion on the temporal basis,  $\{b_l(t); l = 1, \dots, N\}$  are the temporally varying coefficients of the expansion on the spatial basis and  $\{c_{lk}; l = 1, \dots, N; k = 1, \dots, M\}$  are the coefficients of the expansion on the separable spatio-temporal basis.

Various choices for the regularizing terms in space and in time are possible. In this work, following Ramsay [2002], Wood et al. [2008] and Sangalli et al. [2013], we use the spatial roughness penalty

$$J_S(g(\mathbf{p})) = \int_{\Omega} (\Delta g(\mathbf{p}))^2 d\mathbf{p}, \quad (5)$$

where  $g : \Omega \rightarrow \mathbb{R}$  and the Laplacian  $\Delta g(\mathbf{p}) = \frac{\partial^2 g}{\partial x^2}(\mathbf{p}) + \frac{\partial^2 g}{\partial y^2}(\mathbf{p})$  provides a simple measure of the local curvature of  $g$ . Other possible choices for spatial roughness penalties are, for instance, that associated with thin plate splines, given by  $\int_{\mathbb{R}^2} (\frac{\partial^2 g}{\partial x^2}(\mathbf{p}))^2 + 2(\frac{\partial^2 g}{\partial x \partial y}(\mathbf{p}))^2 + (\frac{\partial^2 g}{\partial y^2}(\mathbf{p}))^2 d\mathbf{p}$ , or a penalization involving more complex partial differential operators describing prior knowledge on the phenomenon under study (see, e.g., Azzimonti et al. [2014]).

There are several possibilities for the temporal roughness penalties. We adopt the classical penalty

$$J_T(h(t)) = \int_{T_1}^{T_2} \left( \frac{d^r h(t)}{dt^r} \right)^2 dt \quad (6)$$

where  $h : [T_1, T_2] \rightarrow \mathbb{R}$ . See, e.g., Ramsay and Silverman [2005], Chapter 5, for details.

In analogy to the models developed by Augustin et al. [2013] and Marra et al. [2012], the spatial penalty  $J_S$  is directly applied to the  $M$  spatially varying coefficients  $a_k(\mathbf{p})$  in the basis expansion (2), and the temporal penalty  $J_T$  is directly applied to the  $N$  temporally varying coefficients  $b_l(t)$  in the basis expansion (3). The field  $f$  is thus estimated by minimizing the following penalized sum of square error criterion:

$$J(f) = \sum_{i=1}^n \sum_{j=1}^m (z_{ij} - f(\mathbf{p}_i, t_j))^2 + \lambda_S \sum_{k=1}^M \int_{\Omega} (\Delta(a_k(\mathbf{p})))^2 d\mathbf{p} + \lambda_T \sum_{l=1}^N \int_{T_1}^{T_2} \left( \frac{d^r b_l(t)}{dt^r} \right)^2 dt, \quad (7)$$

where  $\lambda_S > 0$  and  $\lambda_T > 0$  are two smoothing parameters that weight the penalizations respectively in space and time. The choice of these parameters will be discussed in Section 3.3. The Appendix provides further explanation for the form of the penalized sum of square error functional  $J$  here considered.

## 3 Numerical implementation of the model

### 3.1 Choice of the basis systems in space and time

Various possible bases can be used for the expansions in the spatial and temporal domains. In this work, we use in space a finite element basis on a triangulation  $\Omega_{\tau}$  of the spatial domain  $\Omega$  of interest. This choice leads to a efficient

discretization of the functional  $J$  and allows an accurate account of the shape of the spatial domain.

We illustrate the construction of such basis on Venice domain. Before building the basis, we simplify the original spatial domain represented in Figure 1, excluding the coastal uninhabited regions and the smaller islands, and keeping in the domain of study only the four major islands: Venice, Murano (at the north-east of Venice), Lido di Venezia (at the south-east of Venice) and Pellestrina (at the south of Lido). We then smooth the boundary of the domain with regression splines. Finally, we obtain a piecewise linear boundary, sub-sampling from this smooth curve so that the features characterizing the domain are preserved. Figure 4 shows the simplified boundary of Venice province, while Figure 5 shows the detail around the city of Venice. This region is particularly interesting since it shows the four islands we keep in the domain. Here the domain includes four bridges: one linking Venice to the continent and the others linking some of the islands between themselves; the first one is an actual bridge with a road and a railway, while the other bridges represent regular and frequent ferries among the islands.



Figure 4: Simplified boundary of the Venice province.

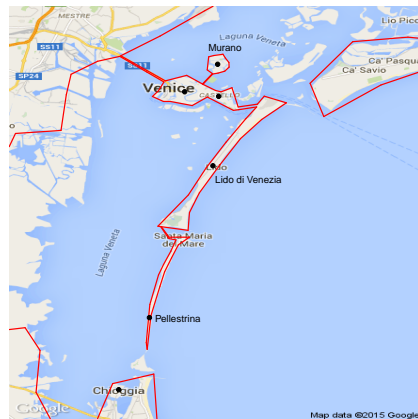


Figure 5: Detail of the simplified boundary of the Venice province.

A triangulation of the resulting simplified domain is then obtained using the R package RTriangle [Shewchuk, 1996]. In particular, we start from a Delaunay triangulation, constrained within the simplified boundary, where each of the town locations and each point defining the simplified boundary become a triangle vertex. A more regular mesh is then obtained with additional vertices, imposing a maximum value to the triangle areas. Figure 6 displays the resulting triangulation of Venice province. For this application, here and in Section 6, instead of using as coordinates the latitude and longitude, we employ the UTM coordinate system, which allows to compute the distance between two points on the Earth's surface by means of the Euclidean distance instead of the geodesic distance.



Figure 6: Triangulation of the Venice province.

The finite element basis is composed by globally continuous functions that coincides with a polynomial of a certain degree on each element of the domain triangulation. In particular we use here a linear finite element basis, which is composed by piecewise linear basis functions. Each basis function is associated to a vertex of the triangulation, and has value 1 at that vertex and 0 at all other vertices. Figure 7 shows an example of linear basis function.

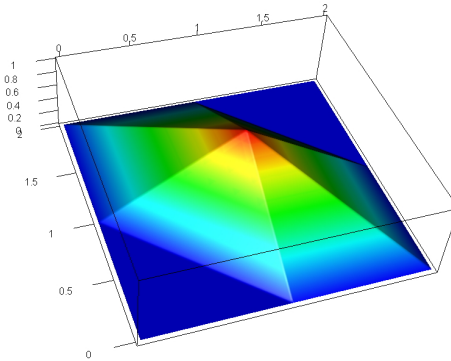


Figure 7: Example of linear finite element basis function.

We use a cubic B-spline basis for time with penalization of the second derivative. Other basis systems may turn out to be more appropriate in other applicative contexts. For instance, Fourier basis are well suited to the case of cyclic data, possibly with penalization of the harmonic acceleration operator, instead of the order  $r$  derivative considered in (6).

### 3.2 Discretization of the penalized sum-of-square error functional

Let  $\mathbf{z}$  be the vector of length  $nm$  of observed values at the  $n \times m$  spatio-temporal locations,  $\mathbf{f}$  the vector of length  $nm$  of evaluations of the spatio-temporal function  $f$  at the  $n \times m$  spatio-temporal locations, and  $\mathbf{c}$  the vector of length  $NM$  of

coefficients of the basis expansion (4) of the spatio-temporal field  $f$ , with entries ordered as follows

$$\mathbf{z} = \begin{bmatrix} z_{11} \\ \vdots \\ z_{1m} \\ z_{21} \\ \vdots \\ z_{2m} \\ \vdots \\ z_{nm} \end{bmatrix} \quad \mathbf{f} = \begin{bmatrix} f(\mathbf{p}_1, t_1) \\ \vdots \\ f(\mathbf{p}_1, t_m) \\ f(\mathbf{p}_2, t_1) \\ \vdots \\ f(\mathbf{p}_2, t_m) \\ \vdots \\ f(\mathbf{p}_n, t_m) \end{bmatrix} \quad \mathbf{c} = \begin{bmatrix} c_{11} \\ \vdots \\ c_{1M} \\ c_{21} \\ \vdots \\ c_{2M} \\ \vdots \\ c_{NM} \end{bmatrix}.$$

Let  $\Psi$  be the  $n \times N$  matrix of the evaluations of the  $N$  spatial basis functions in the  $n$  space locations  $\{\mathbf{p}_i; i = 1, \dots, n\}$ ,

$$\Psi = \begin{bmatrix} \psi_1(\mathbf{p}_1) & \psi_2(\mathbf{p}_1) & \dots & \psi_N(\mathbf{p}_1) \\ \psi_1(\mathbf{p}_2) & \psi_2(\mathbf{p}_2) & \dots & \psi_N(\mathbf{p}_2) \\ \vdots & \vdots & \dots & \vdots \\ \psi_1(\mathbf{p}_n) & \psi_2(\mathbf{p}_n) & \dots & \psi_N(\mathbf{p}_n) \end{bmatrix}.$$

Moreover, define the vectors of length  $N$  of the spatial basis functions  $\boldsymbol{\psi}$ , and of their first order partial derivatives  $\boldsymbol{\psi}_x$  and  $\boldsymbol{\psi}_y$ , by

$$\boldsymbol{\psi} = \begin{bmatrix} \psi_1 \\ \psi_2 \\ \vdots \\ \psi_N \end{bmatrix} \quad \boldsymbol{\psi}_x = \begin{bmatrix} \partial\psi_1/\partial x \\ \partial\psi_2/\partial x \\ \vdots \\ \partial\psi_N/\partial x \end{bmatrix} \quad \boldsymbol{\psi}_y = \begin{bmatrix} \partial\psi_1/\partial y \\ \partial\psi_2/\partial y \\ \vdots \\ \partial\psi_N/\partial y \end{bmatrix}.$$

Analogously, let  $\Phi$  be the  $m \times M$  matrix of the evaluations of the  $M$  temporal basis functions in the  $m$  time instants  $\{t_j; j = 1, \dots, m\}$ :

$$\Phi = \begin{bmatrix} \varphi_1(t_1) & \varphi_2(t_1) & \dots & \varphi_M(t_1) \\ \varphi_1(t_2) & \varphi_2(t_2) & \dots & \varphi_M(t_2) \\ \vdots & \vdots & \dots & \vdots \\ \varphi_1(t_m) & \varphi_2(t_m) & \dots & \varphi_M(t_m) \end{bmatrix}.$$

Moreover, define the vectors of length  $M$  of the temporal basis functions  $\boldsymbol{\varphi}$ , and of their second order derivatives  $\boldsymbol{\varphi}_{tt}$ , by

$$\boldsymbol{\varphi} = \begin{bmatrix} \varphi_1 \\ \varphi_2 \\ \vdots \\ \varphi_M \end{bmatrix} \quad \boldsymbol{\varphi}_{tt} = \begin{bmatrix} d^2\varphi_1/dt^2 \\ d^2\varphi_2/dt^2 \\ \vdots \\ d^2\varphi_M/dt^2 \end{bmatrix}.$$

Consider the  $nm \times NM$  matrix  $B = \Psi \otimes \Phi$ , where  $\otimes$  denotes the Kronecker product. Then  $\mathbf{f} = B\mathbf{c}$ . Moreover, denote by  $I_K$  the identity matrix of dimension  $K$ . Then, we may rewrite the sum of square error functional  $J$  in (7) as

$$\begin{aligned} J &= (\mathbf{z} - B\mathbf{c})^T (\mathbf{z} - B\mathbf{c}) + \lambda_S \mathbf{c}^T (P_S \otimes I_M) \mathbf{c} + \lambda_T \mathbf{c}^T (I_N \otimes P_T) \mathbf{c} \\ &= (\mathbf{z} - B\mathbf{c})^T (\mathbf{z} - B\mathbf{c}) + \mathbf{c}^T P \mathbf{c}, \end{aligned} \quad (8)$$

where  $P_S$  and  $P_T$  are the matrix discretizations of the integrals of the spatial and temporal penalization terms, and  $P$  is the overall penalty  $P = \lambda_S (P_S \otimes I_M) + \lambda_T (I_N \otimes P_T)$ .

The matrix  $P_T$  is obtained by direct discretization of the temporal penalty term in (6) and (7):

$$P_T = \int_{T_1}^{T_2} \varphi_{tt} \varphi_{tt}^T;$$

see Ramsay and Silverman [2005] for details. For the matrix  $P_S$ , following Ramsay [2002] and Sangalli et al. [2013], we consider a computationally efficient discretization of the spatial penalty term in (5) and (7), that does not involve the computation of second order derivatives of the basis functions, but only of first order derivatives. This discretization is given by  $P_S = R_1 R_0^{-1} R_1$ , where

$$R_0 = \int_{\Omega_\tau} \psi \psi^T, \quad R_1 = \int_{\Omega_\tau} (\psi_x \psi_x^T + \psi_y \psi_y^T),$$

and it is based on a variational characterization of the estimation problem; see Ramsay [2002] for details. This formulation uses the Neumann condition at the boundary of the domain of interest implying zero flow across the boundary. Various other boundary conditions are possible; see Sangalli et al. [2013]. As shown in Azzimonti et al. [2014], in the finite element space used to discretize the problem, the matrix  $P_S$  is in fact equivalent to the penalty matrix that would be obtained as direct discretization of the penalty term in (5) and (7) and involving the computation of second order derivatives.

Finally, the coefficients vector  $\hat{\mathbf{c}}$  that minimizes the functional  $J$  in (8) is computed deriving  $J$  with respect to  $\mathbf{c}$  and setting the derivative equal to 0, obtaining

$$\hat{\mathbf{c}} = (B^T B + P)^{-1} B^T \mathbf{z}.$$

### 3.3 Properties of the estimator

The estimator  $\hat{\mathbf{c}}$  is linear in the observed data values  $\mathbf{z}$ , and has a typical penalized least-square form. Since  $E[\mathbf{z}] = \mathbf{f}$  and  $Var[\mathbf{z}] = \sigma^2 I_{nm}$ , we obtain

$$\begin{aligned} E[\hat{\mathbf{c}}] &= (B^T B + P)^{-1} B^T \mathbf{f}, \\ Var[\hat{\mathbf{c}}] &= \sigma^2 (B^T B + P)^{-1} B^T B (B^T B + P)^{-1}. \end{aligned}$$

Consider the vector  $\mathbf{B}(\mathbf{p}, t) = \psi(\mathbf{p})^T \otimes \varphi(t)^T$  of evaluations of the separable basis system at the spatio-temporal location  $(\mathbf{p}, t)$ , with  $\mathbf{p} \in \Omega$  and  $t \in [T_1, T_2]$ . The estimate of the field  $f$  at this generic location is thus given by

$$\hat{f}(\mathbf{p}, t) = \mathbf{B}(\mathbf{p}, t) \hat{\mathbf{c}} = \mathbf{B}(\mathbf{p}, t) (B^T B + P)^{-1} B^T \mathbf{z}$$

and its mean and expected values are given by

$$\begin{aligned} E[\hat{f}(\mathbf{p}, t)] &= \mathbf{B}(\mathbf{p}, t) (B^T B + P)^{-1} B^T \mathbf{f} \\ Var[\hat{f}(\mathbf{p}, t)] &= \sigma^2 \mathbf{B}(\mathbf{p}, t) (B^T B + P)^{-1} B^T B (B^T B + P)^{-1} \mathbf{B}(\mathbf{p}, t)^T. \end{aligned} \tag{9}$$

The smoothing matrix

$$S = B (B^T B + P)^{-1} B^T$$

maps the vector of observed values  $\mathbf{z}$  to the vector of fitted values  $\hat{\mathbf{z}} = \hat{\mathbf{f}} = S\mathbf{z}$ . The trace of the smoothing matrix constitutes a commonly used measure of the equivalent degrees of freedom for linear estimators. We can thus estimate  $\sigma^2$  by

$$\hat{\sigma}^2 = \frac{1}{nm - \text{tr}(S)} (\mathbf{z} - \hat{\mathbf{z}})^T (\mathbf{z} - \hat{\mathbf{z}}). \quad (10)$$

This estimate of the error variance, plugged into (9), can be used to compute approximate pointwise confidence intervals for  $f$ . Moreover, the value of a new observation at location point  $\mathbf{p}_{n+1}$  and time instant  $t_{m+1}$  can be predicted by  $\hat{z}_{n+1, m+1} = \hat{f}(\mathbf{p}_{n+1}, t_{m+1})$ , and approximate prediction intervals may be constructed.

Finally, the values of the smoothing parameters  $\lambda_S$  and  $\lambda_T$  may be chosen via Generalized Cross-Validation (GCV), searching for the values of  $\lambda_S, \lambda_T$  that minimize

$$GCV(\lambda_S, \lambda_T) = \frac{nm}{(nm - \text{tr}(S))^2} (\mathbf{z} - \hat{\mathbf{z}})^T (\mathbf{z} - \hat{\mathbf{z}}).$$

## 4 Model with covariates

The model described above can be easily extended to include space-time varying covariates. Consider the semi-parametric generalized additive model

$$z_{ij} = \mathbf{w}_{ij}^T \boldsymbol{\beta} + f(\mathbf{p}_i, t_j) + \epsilon_{ij} \quad i = 1, \dots, n, \quad j = 1, \dots, m, \quad (11)$$

where  $\mathbf{w}_{ij}$  is a vector of  $q$  covariates associated to the observation  $z_{ij}$ , at location  $\mathbf{p}_i$  and time instant  $t_j$ , and  $\boldsymbol{\beta}$  is a vector of  $q$  regression coefficients. We can jointly estimate the vector of regression coefficient  $\boldsymbol{\beta}$  and the spatio-temporal field  $f$  by minimizing the following penalized sum of square errors criterion

$$J(f, \boldsymbol{\beta}) = \sum_{i=1}^n \sum_{j=1}^m (z_{ij} - \mathbf{w}_{ij}^T \boldsymbol{\beta} - f(\mathbf{p}_i, t_j))^2 + \lambda_S \sum_{k=1}^M \int_{\Omega} (\Delta(a_k(\mathbf{p})))^2 d\mathbf{p} + \lambda_T \sum_{l=1}^N \int_{T_1}^{T_2} \left( \frac{d^2 b_l(t)}{dt^2} \right)^2 dt. \quad (12)$$

Let  $W$  be the  $nm \times q$  matrix containing the vectors  $\{\mathbf{w}_{ij}; i = 1, \dots, n; j = 1, \dots, m\}$ :

$$W = \begin{bmatrix} \mathbf{w}_{11}^T \\ \mathbf{w}_{12}^T \\ \vdots \\ \mathbf{w}_{1m}^T \\ \mathbf{w}_{21}^T \\ \vdots \\ \mathbf{w}_{2m}^T \\ \vdots \\ \mathbf{w}_{nm}^T \end{bmatrix}.$$

Let  $H_W$  be the matrix that projects orthogonally on the space generated by the columns of  $W$ , i.e.  $H_W = W(W^T W)^{-1} W^T$  and let  $Q = I_{nm} - H_W$ . The

discretization of the functional  $J(f, \boldsymbol{\beta})$  in (12) is given by

$$J = (\mathbf{z} - W\boldsymbol{\beta} - B\mathbf{c})^T (\mathbf{z} - W\boldsymbol{\beta} - B\mathbf{c}) + \mathbf{c}^T P\mathbf{c} .$$

To compute the estimates of the vector of regression coefficients  $\boldsymbol{\beta}$  and of the vector  $\mathbf{c}$  of coefficients of the basis expansion of the spatio-temporal field  $f$ , we compute the first partial derivatives of  $J$  with respect to  $\boldsymbol{\beta}$  and  $\mathbf{c}$ , and set them equal to zero, getting the following explicit solution of the estimation problem:

$$\begin{aligned} \hat{\boldsymbol{\beta}} &= (W^T W)^{-1} W^T (\mathbf{z} - B\hat{\mathbf{c}}), \\ \hat{\mathbf{c}} &= (B^T Q B + P)^{-1} B^T Q \mathbf{z}. \end{aligned}$$

The estimator  $\hat{\mathbf{c}}$  has a penalized least-square form; given  $\hat{\mathbf{c}}$ , the estimator  $\hat{\boldsymbol{\beta}}$  has a least square form.

#### 4.1 Properties of the estimator

Let  $S_{\mathbf{f}} = B(B^T Q B + P)^{-1} B^T Q$ , so that

$$\hat{\boldsymbol{\beta}} = (W^T W)^{-1} W^T (I - S_{\mathbf{f}}) \mathbf{z}.$$

Since  $E[\mathbf{z}] = W\boldsymbol{\beta} + \mathbf{f}$  and  $Var[\mathbf{z}] = \sigma^2 I_{nm}$ , and exploiting the fact that the matrix  $Q$  is idempotent and  $QW = 0$ , we obtain

$$\begin{aligned} E[\hat{\mathbf{c}}] &= (B^T Q B + P)^{-1} B^T Q \mathbf{f}, \\ Var[\hat{\mathbf{c}}] &= \sigma^2 (B^T Q B + P)^{-1} B^T Q B (B^T Q B + P)^{-1} \end{aligned}$$

and

$$\begin{aligned} E[\hat{\boldsymbol{\beta}}] &= \boldsymbol{\beta} + (W^T W)^{-1} W^T (I - S_{\mathbf{f}}) \mathbf{f} \\ Var[\hat{\boldsymbol{\beta}}] &= \sigma^2 (W^T W)^{-1} + \sigma^2 (W^T W)^{-1} W^T S_{\mathbf{f}} S_{\mathbf{f}}^T W (W^T W)^{-1}. \end{aligned} \tag{13}$$

The estimate of the field  $f$  and its distributional properties follow as for the model without covariates. The smoothing matrix  $S$ , such that  $\hat{\mathbf{z}} = S\mathbf{z}$ , is now given by

$$S = H_W + Q S_{\mathbf{f}}.$$

The trace of this matrix is given by  $tr(S) = q + tr(S_{\mathbf{f}})$  and measures the edf of this estimator, given by the sum of the  $q$  degrees of freedom corresponding to the parametric part of the model and the  $tr(S_{\mathbf{f}})$  degrees of freedom corresponding to the non-parametric part of the model. We can estimate  $\sigma^2$  as in (10). Given this estimate, it is possible to construct approximate pointwise confidence intervals for  $f$  as in the case without covariates. Moreover, using  $\hat{\sigma}^2$  in (13), it is now also possible to compute approximate confidence intervals for  $\boldsymbol{\beta}$ . Finally, the value of a new observation at location point  $\mathbf{p}_{n+1}$  and time instant  $t_{m+1}$  and with associated covariates  $\mathbf{w}_{n+1 \ m+1}$  can be predicted by  $\hat{z}_{n+1 \ m+1} = \mathbf{w}_{n+1 \ m+1}^T \hat{\boldsymbol{\beta}} + \hat{f}(\mathbf{p}_{n+1}, t_{m+1})$ , and approximate prediction intervals may be constructed.

## 5 Simulation studies

We present some simulation studies and compare the proposed model with three other approaches to spatio-temporal field estimation.

The first method is spatio-temporal kriging with a separable variogram marginally gaussian in space and exponential in time, chosen among a number of possible variogram models, with parameters estimated from the empirical variogram. This method is implemented using the function `krigeST` of the R package `gstat` [Pebesma, 2004]. We then consider two separable space-time models presented in Augustin et al. [2013] and Marra et al. [2012]. One model adopt a thin plate spline basis in space and a cubic spline basis in time, and minimizes a functional analogous to (7), where the spatial penalty is replaced by the thin plate spline energy recalled in Section 2. The other model uses the soap film smoothing described in Wood et al. [2008] in space and a cubic spline basis in time, and minimize the same functional in (7). The two latter methods are implemented using the function `gam` of the R package `mgcv` [Wood, 2006]. Finally, for these two methods, as well as for the model here proposed, the values of the smoothing parameters  $\lambda_S, \lambda_T$  are chosen via GCV.

### 5.1 Simulation study without covariates

We apply the methods to simulated data on a C-shaped spatial domain, considering the spatial test function  $g$ , used for instance in Ramsay [2002], Wood et al. [2008] and Sangalli et al. [2013], that is shown in the top left panel of Figure 8. We then construct a spatio-temporal test function  $f$  in the following way:  $f(\mathbf{p}, t) = g(\mathbf{p}) \cos(t)$ . We sample 200 spatial locations uniformly in the C-shaped domain at 9 time instants equally spaced from 0 to  $\pi$ . We simulate the data from model (1), with a gaussian noise with mean 0 and standard deviation 1.

Figure 8 shows in the first column the spatio-temporal test function at five time instants, in the second column the simulated data, and in the following columns the corresponding estimates obtained by spatio-temporal kriging (KRIG), the separable space-time model using thin plate spline (TPS), the separable space-time model using soap film smoothing (SOAP), and the separable space-time model here proposed (ST-PDE).

Figure 9 shows the boxplots of the Root Mean Square Errors (RMSE) of the space-time field estimates given by the four methods over 50 replicates of the noise generation. The RMSE is computed over a fine grid of the spatio-temporal domain (step 0.05 in space and  $\pi/24$  in time).

A visual inspection of the RMSE shows that SOAP and ST-PDE methods give better estimates than KRIG and TPS. The reason for this comparative advantage is apparent from Figure 8. In fact, the KRIG and TPS methods, that do not take into account the shape of the domain and smooth across the two arms of the C-shaped domain, provide poor estimates of the field when the true  $f$  is characterized by high values in one of the two C arms and low values in the other arm. The best estimates are provided by the ST-PDE model.

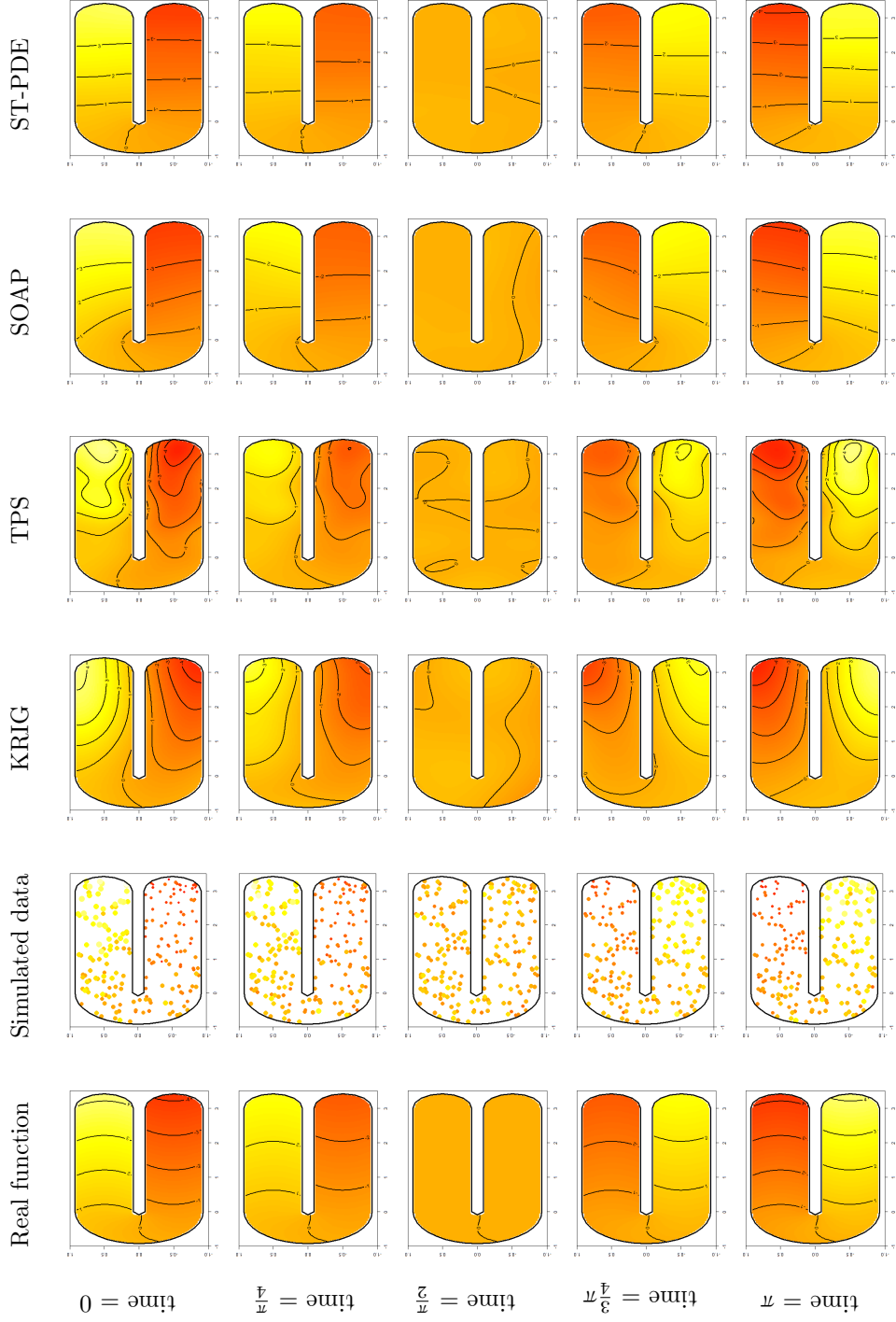


Figure 8: The spatio-temporal test function, the simulated data and the estimated functions with spatio-temporal kriging (KRIG), separable space-time model using thin plate spline (TPS), separable space-time model using soap film smoothing (SOAP) and ST-PDE.

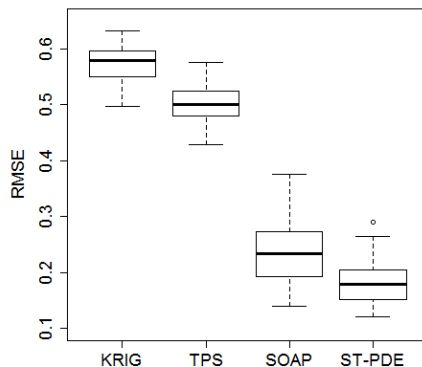


Figure 9: Simulation study without covariates. Boxplots of the RMSE of the estimates of the spatio-temporal field obtained by the four tested methods: spatio-temporal kriging (KRIG), separable space-time model using thin plate spline (TPS), separable space-time model using soap film smoothing (SOAP) and ST-PDE.

## 5.2 Simulation study with covariates

Within the same simulation setting described in Section 5.1, we also perform a study including space-time varying covariates. Specifically, for each simulation replicates, independently for each data location  $\mathbf{p}_i$  and time instant  $t_j$ , we sample a covariate  $w_{ij}$  from a normal distribution, with mean 0 and variance 1. We then generate data from model (11), setting  $\beta = 1$ . The other simulation specifications are as in Section 5.1. We here compare the proposed ST-PDE method to the separable space-time model using thin plate spline (TPS) and separable space-time model using soap film smoothing (SOAP). We do not instead consider the spatio-temporal kriging because the function `krigeST` of the R package `gstat` cannot handle covariates.

Figure 10 shows the boxplots of the Root Mean Square Errors (RMSE) of the space-time field estimate over the 50 simulation replicates. The RMSE is computed over the same fine grid of the spatio-temporal domain used in Section 5.1. Likewise in the simulation study without covariates, SOAP and ST-PDE, that account for the shape of the domain, provide better estimates than TPS, that is instead blind to the domain structure. The best estimates are provided by the ST-PDE model.

The RMSE of the estimates of  $\beta$  over the 50 replicates are instead comparable for the three methods: 0.025 for TPS, 0.024 for both SOAP and ST-PDE. In the first simulation replicate, the approximate 95% confidence interval for the parameter  $\beta$  associated to the ST-PDE estimate is given by [0.99, 1.09].

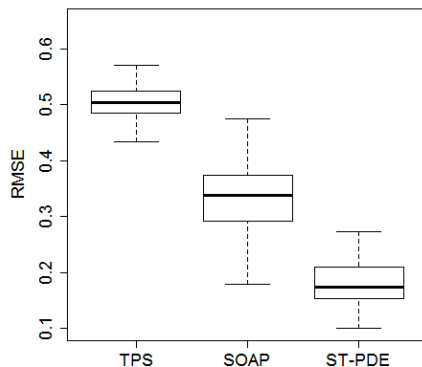


Figure 10: Simulation study with covariates. Boxplots of the RMSE of the estimates of the spatio-temporal field obtained by the three methods tested: separable space-time model using thin plate spline (TPS), separable space-time model using soap film smoothing (SOAP) and ST-PDE.

## 6 Application to the analysis of the production of waste in Venice province

We apply the ST-PDE method to the dataset of annual amount of per capita municipal waste produced in the Venice province.

### 6.1 The Venice waste dataset

Open Data Veneto<sup>1</sup> provides the gross and per capita annual amount of municipal waste produced in each municipality of the Venice province in the period from 1997 to 2011. We here consider for the analysis the annual yearly per capita municipal waste, in kg per municipality resident.

Municipal waste includes that produced in houses and public areas, but does not include special waste, i.e. industrial, agricultural, construction and demolition waste, or hazardous waste, for which there are special disposal programs. Therefore, the data refer only to the urban area of the municipality, whilst they do not refer to the agricultural or industrial areas in the municipality territories. Since no data identifying the urbanized areas of the municipalities is available, we face here two possible simplifications of the problem. We can either partition the Venice province in the municipality territories and attribute each datum to the whole territory of its municipality, or assign each datum to a point representing the center of the municipality. We here adopt the second simplification. The spatial coordinates of the town centers are available online<sup>2</sup>. As mentioned in Section 3, latitude and longitude are converted into UTM coordinate system.

In some cases there are localities which do not constitute a municipality on their own, but are under the jurisdiction of another town. Some of these localities are not negligible for the problem under analysis due to their tourist relevance and their location on the domain; for this reason we add them to the

<sup>1</sup><http://dati.veneto.it/dataset/produzione-annua-di-rifiuti-urbani-totale-e-pro-capite-1997-2011>

<sup>2</sup><http://www.dossier.net/utilities/coordinate-geografiche/>

data. Specifically, we include the seaside town of Bibione, the eastern most village indicated in Figure 1. This popular vacation destination falls under the jurisdiction of the municipality of San Michele al Tagliamento, north west of Bibione; the waste data considered for Bibione are a replicate of the data of San Michele al Tagliamento. Moreover, we replicate the data of Venice in the islands of Murano, Lido di Venezia and Pellestrina, because of their tourist relevance and the particular shape of the domain.

Since intuition suggests that the production of waste is affected by tourism, we include in the model a covariate which accounts for it. Specifically we consider the number of beds in accommodation facilities (such as hotels, bed and breakfast, guest houses, campings, etc.) divided by the number of residents. This ratio may be as large as 7 in some tourist towns by the sea. The number of beds in accommodation facilities is provided by Istat<sup>3</sup>, the Italian national institute for statistics.

## 6.2 Analysis of Venice waste data by ST-PDE

Figure 11 shows the estimated spatio-temporal field at fixed time instants. The estimate for the coefficient  $\beta$  is 30.56 meaning that one more unit in the ratio between the number of beds in accommodation facilities and the number of residents is estimated to increase the yearly per capita production of waste by residents by about 30kg. The estimated spatial field  $f$  shows the highest values, across the years, in correspondence of the coastline, around the towns of Bibione, Lido di Jesolo and Cavallino-Treporti. These higher values may be due to a type of tourism that is not captured by the available covariate, such as daily tourists who do not stay overnight, and vacationers who either own or rent vacation houses. The higher values of the field are also probably due to the presence of many seasonal workers, working in accommodation facilities, restaurants, cafés, shops, beach resorts and other services, who are not residents of these towns.

Although Venice is one of the most visited cities in Italy, and this tourism is active all year round, the production of per capita waste in Venice appears to be lower than in other nearby tourist localities by the seaside. This might be partly explained by the fact that the tourist activities in Venice are not so highly characterized by seasonality as in the smaller seaside villages, and people working in tourist activities in Venice are more likely to be themselves residents of this large city.

---

<sup>3</sup><http://www.istat.it/it/archivio/113712>

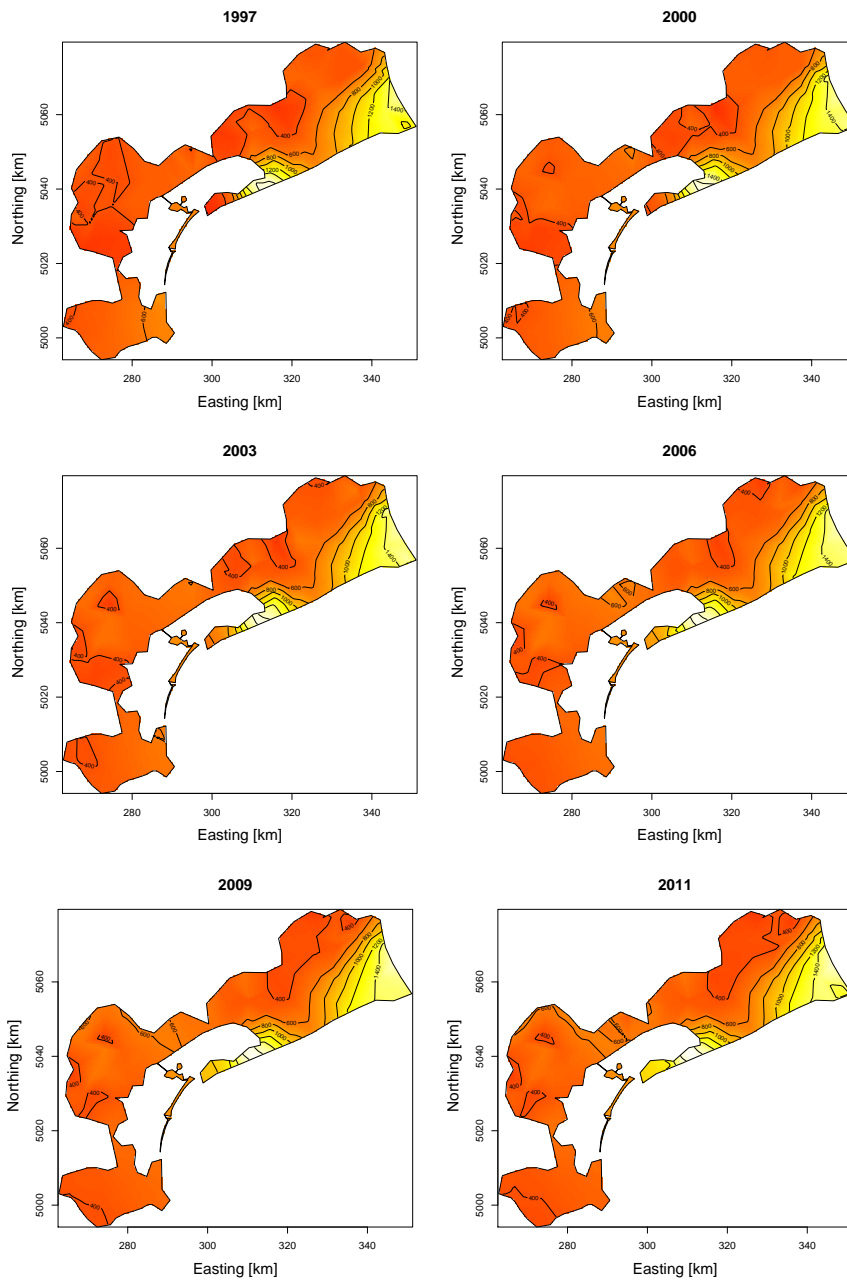


Figure 11: Estimated spatio-temporal field for the Venice waste data (yearly per capita production) at fixed time instants.

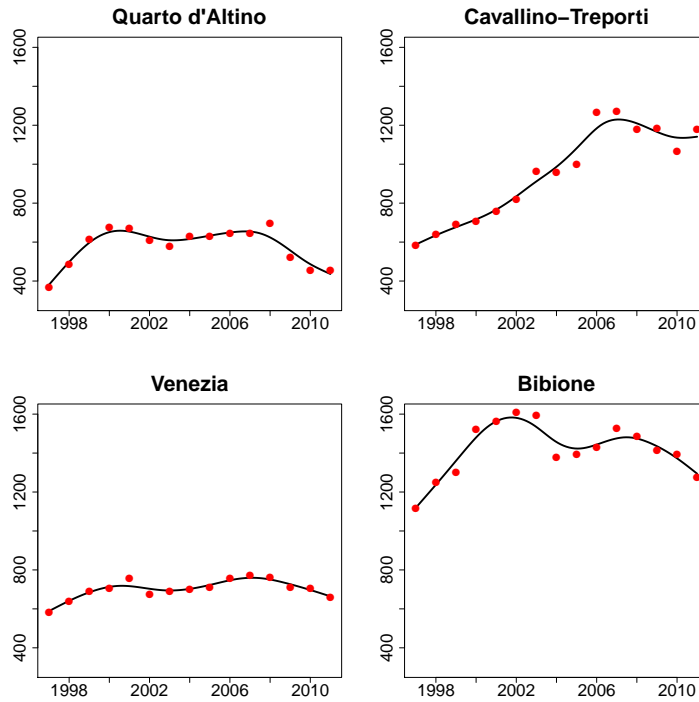


Figure 12: Temporal evolution of the estimated spatio-temporal field for the Venice waste data (yearly per capita production) at fixed spatial locations.

It is significant to notice how the estimated function does not smooth across concave boundaries. For example, the area of the city of Quarto d'Altino and the one around the city of Cavallino-Treporti show different ranges of values. Indeed, even though the two towns are geographically close, they are separated by the Venetian lagoon. This difference is evident also from the first two panels of Figure 12, which shows the estimated spatio-temporal field at fixed localities: Quarto d'Altino, Cavallino-Treporti, Venice and Bibione. In these plots the red dots are obtained subtracting from the data the estimated contribution by the covariate, i.e.  $\hat{\beta}w_{ij}$ .

The temporal evolution plots in Figure 12 show the ability of the method to capture the temporal trend of the phenomenon. The method provides good estimates also for the municipality of Cavallino-Treporti, which presents a strong variation of per capita waste over the year. The large increase of the per capita waste of Cavallino-Treporti is partly explained by the fact that, during the first years of this study, this town was under the jurisdiction of Venice, while the data for this new municipality are available only from 2002. In particular, the data for Cavallino-Treporti for years 1997 to 2001 are a replicate of the data of the municipality of Venice. Nevertheless, the strong variation in the data is well captured by the estimated function.

## 7 Model extensions

Various extensions of the proposed model are possible. Areal data can be handled similarly to [Azzimonti et al. \[2014\]](#). Following the approach presented in the latter work, it is also possible to include a priori information available on the phenomenon under study, using more complex differential regularizations modelling the space and time behavior of the phenomenon. This also allows to account for non-stationarities and anisotropies in space and time. Along the same lines, a non-separable version of the model, with a unique regularization that jointly involves space and time, could be considered. Finally, data distributed over curved domains, instead of over planar domains, could be handled as described in [Ettinger et al. \[2012\]](#).

**Acknowledgments:** We are grateful to Alessandra Menafoglio for interesting discussion on this work.

## Appendix

### A About the penalized sum of square error criterion

Ideally, we would like to estimate the spatio-temporal field  $f(\mathbf{p}, t)$  minimizing the following penalized sum of square error criterion

$$\begin{aligned} \tilde{J}(f) = & \sum_{i=1}^n \sum_{j=1}^m (z_{ij} - f(\mathbf{p}_i, t_j))^2 + \\ & + \lambda_S \int_{T_1}^{T_2} \int_{\Omega} (\Delta f(\mathbf{p}, t))^2 d\mathbf{p} dt + \lambda_T \int_{\Omega} \int_{T_1}^{T_2} \left( \frac{\partial^2 f(\mathbf{p}, t)}{\partial t^2} \right)^2 dt d\mathbf{p}, \end{aligned} \quad (14)$$

where the spatial and temporal penalties are applied to the function  $f(\mathbf{p}, t)$  and integrated, respectively, over the temporal and spatial domain.

We here show that the functional  $J(f)$  in (7) constitutes indeed the discretization of the functional  $\tilde{J}(f)$  in (14) if the field  $f$  is represented by a separable space-time basis expansion where both the spatial and the temporal basis systems are orthonormal.

In fact, using the basis expansion for  $f$  given in (2), we can rewrite the

spatial penalty in (14) as follows

$$\begin{aligned}
\int_{T_1}^{T_2} \int_{\Omega} (\Delta f(\mathbf{p}, t))^2 d\mathbf{p} dt &= \int_{T_1}^{T_2} \int_{\Omega} \left( \Delta \left( \sum_{k=1}^M a_k(\mathbf{p}) \varphi_k(t) \right) \right)^2 d\mathbf{p} dt \\
&= \int_{T_1}^{T_2} \int_{\Omega} \left( \sum_{k=1}^M \Delta a_k(\mathbf{p}) \varphi_k(t) \right)^2 d\mathbf{p} dt \\
&= \int_{T_1}^{T_2} \int_{\Omega} \left( \sum_{k=1}^M \Delta a_k(\mathbf{p}) \varphi_k(t) \right) \left( \sum_{h=1}^M \Delta a_h(\mathbf{p}) \varphi_h(t) \right) d\mathbf{p} dt \\
&= \int_{T_1}^{T_2} \int_{\Omega} \left( \sum_{k=1}^M \sum_{h=1}^M \Delta a_k(\mathbf{p}) \Delta a_h(\mathbf{p}) \varphi_k(t) \varphi_h(t) \right) d\mathbf{p} dt \\
&= \sum_{k=1}^M \sum_{h=1}^M \int_{\Omega} \Delta a_k(\mathbf{p}) \Delta a_h(\mathbf{p}) d\mathbf{p} \int_{T_1}^{T_2} \varphi_k(t) \varphi_h(t) dt.
\end{aligned}$$

This discretization is equivalent to the one considered in (7) if the temporal basis is orthonormal, since in this case the quantity  $\int_{T_1}^{T_2} \varphi_k(t) \varphi_h(t) dt$  is equal to 1 if  $k = h$  and 0 otherwise.

Analogously, using the basis expansion for  $f$  given in (3), we can rewrite the temporal penalty (14) as follows

$$\begin{aligned}
\int_{\Omega} \int_{T_1}^{T_2} \left( \frac{\partial^2 f(\mathbf{p}, t)}{\partial t^2} \right)^2 dt d\mathbf{p} &= \int_{\Omega} \int_{T_1}^{T_2} \left( \frac{\partial^2 \sum_{l=1}^N b_l(t) \psi_l(\mathbf{p})}{\partial t^2} \right)^2 dt d\mathbf{p} \\
&= \int_{\Omega} \int_{T_1}^{T_2} \left( \sum_{l=1}^N \frac{d^2 b_l(t)}{dt^2} \psi_l(\mathbf{p}) \right)^2 dt d\mathbf{p} \\
&= \int_{\Omega} \int_{T_1}^{T_2} \left( \sum_{l=1}^N \frac{d^2 b_l(t)}{dt^2} \psi_l(\mathbf{p}) \right) \left( \sum_{h=1}^N \frac{d^2 b_h(t)}{dt^2} \psi_h(\mathbf{p}) \right) dt d\mathbf{p} \\
&= \int_{\Omega} \int_{T_1}^{T_2} \left( \sum_{l=1}^N \sum_{h=1}^N \frac{d^2 b_l(t)}{dt^2} \frac{d^2 b_h(t)}{dt^2} \psi_l(\mathbf{p}) \psi_h(\mathbf{p}) \right) dt d\mathbf{p} \\
&= \sum_{l=1}^N \sum_{h=1}^N \int_{T_1}^{T_2} \frac{d^2 b_l(t)}{dt^2} \frac{d^2 b_h(t)}{dt^2} dt \int_{\Omega} \psi_l(\mathbf{p}) \psi_h(\mathbf{p}) d\mathbf{p}.
\end{aligned}$$

This discretization is equivalent to the one considered in the functional (7) if the spatial basis is orthonormal, since in that case the quantity  $\int_{\Omega} \psi_l(\mathbf{p}) \psi_h(\mathbf{p}) d\mathbf{p}$  is equal to 1 if  $l = h$  and 0 otherwise.

In this work we use basis systems which are computationally efficient but not orthonormal. Nevertheless, the basis systems considered are sparse, so that the terms  $\int_{T_1}^{T_2} \varphi_k(t) \varphi_l(t) dt$  and  $\int_{\Omega} \psi_l(\mathbf{p}) \psi_k(\mathbf{p}) d\mathbf{p}$  are nonzero only for a few couples of indexes  $(l, k)$ .

## References

- N. H. Augustin, V. M. Trenkel, S. N. Wood, and P. Lorance. Space-time modelling of blue ling for fisheries stock management. *Environmetrics*, 24(2): 109–119, 2013.
- L. Azzimonti, L. M. Sangalli, P. Secchi, M. Domanin, and F. Nobile. Blood flow velocity field estimation via spatial regression with PDE penalization. *Journal of the American Statistical Association*, 2014. doi: 10.1080/01621459.2014.946036.
- W. Caballero, R. Giraldo, and J. Mateu. A universal kriging approach for spatial functional data. *Stochastic Environmental Research and Risk Assessment*, 27(7):1553–1563, 2013.
- N. Cressie and C. K. Wikle. *Statistics for spatio-temporal data*. John Wiley & Sons, 2011.
- P. Delicado, R. Giraldo, C. Comas, and J. Mateu. Statistics for spatial functional data: some recent contributions. *Environmetrics*, 21(3-4):224–239, 2010.
- B. Ettinger, S. Perotto, and L. M. Sangalli. Spatial regression models over two-dimensional manifolds. *TechRep. MOX*, 54, 2012.
- R. Giraldo, P. Delicado, and J. Mateu. Ordinary kriging for function-valued spatial data. *Environmental and Ecological Statistics*, 18(3):411–426, 2011.
- M. Goulard and M. Voltz. Geostatistical interpolation of curves: A case study in soil science. In *Geostatistics Tróia'92*, pages 805–816. Springer, 1993.
- R. Ignaccolo, J. Mateu, and R. Giraldo. Kriging with external drift for functional data for air quality monitoring. *Stochastic Environmental Research and Risk Assessment*, 28(5):1171–1186, 2014.
- G. Marra, D. L. Miller, and L. Zanin. Modelling the spatiotemporal distribution of the incidence of resident foreign population. *Statistica Neerlandica*, 66(2): 133–160, 2012.
- A. Menafoglio, P. Secchi, and M. Dalla Rosa. A Universal Kriging predictor for spatially dependent functional data of a Hilbert Space. *Electronic Journal of Statistics*, 7:2209–2240, 2013.
- A. Menafoglio, A. Guadagnini, and P. Secchi. A kriging approach based on Aitchison geometry for the characterization of particle-size curves in heterogeneous aquifers. *Stochastic Environmental Research and Risk Assessment*, 28(7):1835–1851, 2014.
- D. Nerini, P. Monestiez, and C. Manté. Cokriging for spatial functional data. *Journal of Multivariate Analysis*, 101(2):409–418, 2010.
- E. J. Pebesma. Multivariable geostatistics in S: the gstat package. *Computers & Geosciences*, 30:683–691, 2004.
- R Core Team. *R: A Language and Environment for Statistical Computing*. R Foundation for Statistical Computing, Vienna, Austria, 2014. URL <http://www.R-project.org/>.

- J. O. Ramsay and B. W. Silverman. *Functional Data Analysis*. Springer, 2005.
- T. Ramsay. Spline smoothing over difficult regions. *Journal of the Royal Statistical Society: Series B (Statistical Methodology)*, 64(2):307–319, 2002.
- L. M. Sangalli, J. O. Ramsay, and T. O. Ramsay. Spatial spline regression models. *Journal of the Royal Statistical Society: Series B (Statistical Methodology)*, 75(4):681–703, 2013.
- J. R. Shewchuk. Triangle: Engineering a 2d quality mesh generator and delaunay triangulator. In M. C. Lin and D. Manocha, editors, *Applied Computational Geometry: Towards Geometric Engineering*, volume 1148 of *Lecture Notes in Computer Science*, pages 203–222. Springer-Verlag, may 1996. From the First ACM Workshop on Applied Computational Geometry.
- S. Wood. *Generalized additive models: an introduction with R*. CRC press, 2006.
- S. N. Wood, M. V. Bravington, and S. L. Hedley. Soap film smoothing. *Journal of the Royal Statistical Society: Series B (Statistical Methodology)*, 70(5): 931–955, 2008.

## MOX Technical Reports, last issues

Dipartimento di Matematica  
Politecnico di Milano, Via Bonardi 9 - 20133 Milano (Italy)

- 31/2015** Pini, A.; Vantini, S.; Colombo, D.; Colosimo, B. M.; Previtali, B.  
*Domain-selective functional ANOVA for process analysis via signal data: the remote monitoring in laser welding*
- 32/2015** Agasisti, T.; Ieva, F.; Masci, C.; Paganoni, A.M.  
*Does class matter more than school? Evidence from a multilevel statistical analysis on Italian junior secondary school students*
- 33/2015** Fumagalli, A.; Pasquale, L.; Zonca, S.; Micheletti, S.  
*An upscaling procedure for fractured reservoirs with non-matching grids*
- 30/2015** Pini, A.; Vantini, S.  
*Interval-wise testing for functional data*
- 29/2015** Antonietti, P.F.; Cangiani, A.; Collis, J.; Dong, Z.; Georgoulis, E.H.; Giani, S.; Houston, P.  
*Review of Discontinuous Galerkin Finite Element Methods for Partial Differential Equations on Complicated Domains*
- 28/2015** Taffetani, M.; Ciarletta, P.  
*Beading instability in soft cylindrical gels with capillary energy: weakly non-linear analysis and numerical simulations*
- 25/2015** Del Pra, M.; Fumagalli, A.; Scotti, A.  
*Well posedness of fully coupled fracture/bulk Darcy flow with XFEM*
- 27/2015** Marron, J.S.; Ramsay, J.O.; Sangalli, L.M.; Srivastava, A.  
*Functional Data Analysis of Amplitude and Phase Variation*
- 26/2015** Tagliabue, A.; Dede', L.; Quarteroni, A.  
*Nitsche's Method for Parabolic Partial Differential Equations with Mixed Time Varying Boundary Conditions*
- 24/2015** Bonaventura, L:  
*Local Exponential Methods: a domain decomposition approach to exponential time integration of PDE.*